Comparative study of the power transferred from satellite-magnetosphere interactions to auroral emissions

S. L. G. Hess,[1] P. A. Delamere,[1] V. Dols,[1] and L. C. Ray[1]

Received 11 June 2010; revised 30 September 2010; accepted 8 October 2010; published 7 January 2011.

[1] Io's interaction with the Jovian magnetosphere generates a power of about 10^{12} W which propagates as Alfvén waves along the magnetic field lines and is partly transferred to electrons, resulting in intense auroral emissions. A recent study of the power transmission along the Io flux tube and of the electron acceleration at high latitudes showed that the power of the observed emissions is well explained by assuming filamentation of the Alfvén waves in the torus and the acceleration of the electrons at high latitude. At Jupiter, UV footprints related to Europa and Ganymede have also been observed. At Saturn recent observations revealed a weak UV footprint of Enceladus. We apply the Io interaction model to the Europa and Enceladus interactions. We show that the Alfvén wave filamentation leads to a precipitating electron power consistent with the power of the observed UV footprints.

Citation: Hess, S. L. G., P. A. Delamere, V. Dols, and L. C. Ray (2011), Comparative study of the power transferred from satellite-magnetosphere interactions to auroral emissions, *J. Geophys. Res.*, *116*, A01202, doi:10.1029/2010JA015807.

1. Introduction

[2] Satellite-magnetosphere interactions occur when a satellite orbits close to its parent planet, deep inside the planet's magnetosphere. It is characterized by a perturbation of the magnetic field induced by the conducting satellite. This perturbation propagates along the field lines as Alfvén waves [*Neubauer*, 1980; *Goertz*, 1983; *Saur*, 2004] from the satellite to the planet ionosphere, where it generates emissions spanning the spectrum from low-frequency radio to UVs [*Bigg*, 1964; *Connerney et al.*, 1993; *Clarke et al.*, 1996; *Prangé et al.*, 1996; *Clarke et al.*, 2002; *Grodent et al.*, 2009; *Wannawichian et al.*, 2010]. Alfvén waves accelerate electrons that excite the auroral emissions [*Jones and Su*, 2008; *Swift*, 2007; *Hess et al.*, 2007, 2010]. In the Io case, *Hess et al.* [2010] showed that the turbulent filamentation of the Alfvén wave close to the satellite, seen by *Chust et al.* [2005], is necessary to explain the observed power of the emissions. The present paper extends the study of the Alfvén wave propagation and electron acceleration made for the Io-Jupiter interaction by *Hess et al.* [2010] to the Europa-Jupiter and Enceladus-Saturn interactions. We discuss the role of the Alfvén wave filamentation in the interaction between satellites and the surrounding magnetospheres.

[3] The Io-Jupiter interaction is the most well-known case of a magnetosphere-satellite interaction and certainly the most constrained example of auroral phenomenon (see review by *Saur et al.* [2004]). Io is the innermost Galilean satellite of Jupiter, orbiting at 5.95 Jovian radii from the planet's center. Io orbits inside a dense plasma torus which sweeps past Io at a velocity of v_{sat} = 57 km s^{-1}. The background plasma and the frozen in magnetic field (B) corotate, or slightly subcorotate with the planet. This relative motion creates an electric field in the satellite reference frame:

$$E_{sat} = -v_{sat} \times B \tag{1}$$

The electric field induces a current (I) through Io, which likely closes in the Jovian, ultimately generating auroral emissions. The Io footprint aurora was first observed in Infrared by *Connerney et al.* [1993] using a narrowband filter centered on the H_3^+ band near 3.4 μm. *Clarke et al.* [1996] and *Prangé et al.* [1996] reported UV observations of the Io footprint. Many UV observations have since been made, using the Hubble space telescope (HST) [*Clarke et al.*, 2002; *Gérard et al.*, 2006; *Serio and Clarke*, 2008; *Bonfond et al.*, 2007, 2009; *Wannawichian et al.*, 2010].

[4] Several emission spots have been observed in the Jovian ionosphere at latitudes lower than the main auroral oval. The brightest of these spots maps roughly to the position of the footprint of the magnetic field line connecting Jupiter to Io and is thus related to the Io-Jupiter interaction. Other spots have been related to the magnetic footprints of Europa and Ganymede [*Clarke et al.*, 2002; *Grodent et al.*, 2009; *Wannawichian et al.*, 2010]. At Saturn, recent Cassini UVIS observations revealed a weak UV Enceladus footprint [*Pryor et al.*, 2009] after several years searching, with negative results, in UV using HST [*Wannawichian et al.*, 2008].

[5] Ganymede's interaction with the Jovian magnetosphere is different from Io's, because Ganymede has an internal magnetic field, creating a magnetosphere inside the magnetosphere. Because neither Europa nor Enceladus have

[1]LASP, University of Colorado at Boulder, Boulder, Colorado, USA.

0148-0227/11/2010JA015807

Table 1. Summary of Some of the Local Plasma Parameters at Io, Europa, and Enceladus Used in Our Study and the Related Power Generated at These Satellites[a]

Satellite	Magnetic Flux B (nT)	Torus Density (cm^{-3})	Hot Electron Density (cm^{-3})	v_a (km s^{-1})	Σ_A (Ω^{-1})	Generated Power (W)
Io	2000	1500	1	250	2.2	$\sim 10^{12}$
Europa	450	100	1	230	2.4	$\sim 10^{11}$
Enceladus	350	70	0.3	160	3.4	$\sim 3 \times 10^{8}$

[a]From *Bagenal* [1994], *Moncuquet et al.* [2002], *Saur and Strobel* [2005], *Sittler et al.* [2008], and *Fleshman et al.* [2010].

an intrinsic magnetic field, their interaction with the magnetospheres of their respective parent planets is expected to be similar to that of Io with Jupiter.

[6] Studies of the satellite-magnetosphere interactions involve the local satellite-magnetosphere interaction (including nonlinear plasma and magnetic field line flows around the satellite) and the current circuit running along the magnetic field lines and through the planet's ionosphere. In the present paper, we are mainly interested in the second point. The current is generated by the corotational electric field across the satellite. Early models of the interaction assumed a steady state current circuit that ran along the magnetic field lines, and through both the planet and satellite ionospheres (so-called unipolar inductor model [*Goldreich and Lynden-Bell*, 1969]).

[7] However, because a magnetic field line passes the satellite in a few tens of seconds, the transition time for the current circuit along a given field line to reach such a steady state is significantly longer than the overall interaction time. This is particularly true as Alfvén waves, which establish the current circuit, have their velocity (v_a) diminished by the mass density (ρ) of the medium through which they travel:

$$v_a = \frac{B}{\sqrt{\mu_0 \rho + \frac{B^2}{c^2}}} \tag{2}$$

Thus, the dense Io plasma torus slows the Alfvén wave propagation between Io and Jupiter, resulting in a longer bounce time than the transit time of a magnetic field line past Io. This is also the case for Europa and for Enceladus. Even though the plasma density of their respective tori is about ten times lower than Io's, the local magnetic field strength is also several times less than in the Io case. Hence, the Alfvén velocity at Europa and Enceladus is lower than at Io (equation (2)). The mean Alfvén velocity at the satellite is 250 km s^{-1}, 230 km s^{-1}, and 60 km s^{-1} for Io, Europa and Enceladus, respectively (Table 1). Because the current circuit cannot close in the satellite ionosphere, the interaction power is carried by the Alfvén wave (so-called Alfvénic interaction [*Neubauer*, 1980; *Goertz*, 1983; *Saur*, 2004]).

[8] These two regimes, unipolar inductor and Alfvénic interactions, are sometimes presented as two different kinds of interaction, whereas they are two consecutive phases of the same kind of interaction. This is illustrated by the morphology of the Io-related UV auroras [*Gérard et al.*, 2006, Figure 6], which present several spots with decreasing intensities. These spots are understood as the footprints of the Alfvén wave generated at Io, which bounces several times in the torus [*Neubauer*, 1980; *Goertz*, 1983; *Saur*, 2004; *Bonfond et al.*, 2009]. An elongated continuous tail is superimposed with the spots, which is thought to be generated by a steady state current system [*Ergun et al.*, 2009]. In the UV, Io's and Europa's main spot dominates the other features in brightness, which implies that the Alfvén waves carry lots of power.

[9] The tail of the Io footprint, which is several tens of degrees long, emits more power than the main spot although its brightness is far weaker [*Gérard et al.*, 2006]. The power partition between the main spot and the other footprint features of the Europa and Enceladus footprints is not accurately known, mostly because of the very low brightness of their tails. The current system associated with the diffuse tail and the secondary spots involves the nonlinear dispersion of Alfvén waves with time and bounces in the plasma torus and the nonlinear buildup of the steady state current. In the present paper, we limit ourselves to the study of the brighter main spot, which only involves the Alfvén wave packets generated at the satellite propagating directly to the parent planet ionosphere.

[10] The integrated current carried by the Alfvén waves can be obtained from the Ohm voltage-current relation [*Neubauer*, 1980; *Goertz*, 1983; *Saur*, 2004]. For each hemisphere the current is given by:

$$I \sim 2 E_{sat} R_{sat} \Sigma_A \tag{3}$$

where R_{sat} is the satellite radius and Σ_A is the Alfvén conductance given by:

$$\Sigma_A = \sqrt{\frac{\rho}{\mu_0 B^2}} \tag{4}$$

where ρ is the plasma density. The power radiated as Alfvén waves by the satellite-Jupiter interaction is obtained from the electric field across the satellite and the current it generates:

$$P \sim 4 E_{sat}^2 R_{sat}^2 \Sigma_A \tag{5}$$

The exact computation of the generated power must include geometrical considerations as well as an accurate description of the plasma environment of the satellites [*Saur*, 2004]. The power estimates obtained for Io, Europa and Enceladus are $\sim 10^{12}$ W, $\sim 10^{11}$ W, and $\sim 3 \times 10^{8}$ W, respectively (Table 1).

[11] Both the bounce time of the Alfvén wave and the Alfvén wave power are proportional to v_a^{-1} (the latter through Σ_A). This means that low Alfvén velocity ensures a long and intense transition (Alfvénic) regime. Hence, the interactions of Io, Europa and Enceladus with their parent planet's magnetospheres can generate intense Alfvénic auroral spots. This requires that the power of the Alfvén wave packet is efficiently transferred to electrons, which later precipitate into the Jovian ionosphere, collide with ionosphere atoms and generate UV emissions. According to the estimates of the power generated at the satellites, and to the estimates of the power precipitated into the ionosphere

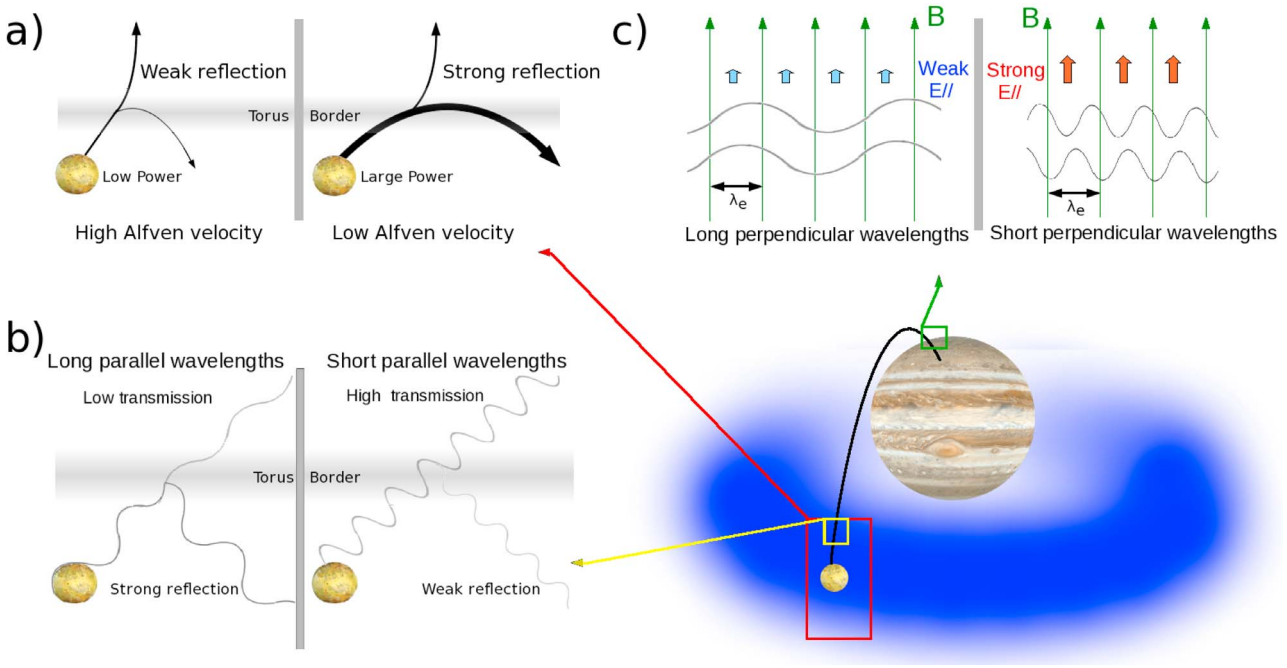

Figure 1. Sketch summarizing the power transfer during the Alfvénic phase of the satellite-magnetosphere interaction. (a) In the case of a large Alfvén velocity near the satellite, the Alfvénic phase is short and does not carry much power. It mostly serves to initiate the following steady state current system. In the case of a low Alfvén velocity near the satellite, the Alfvénic phase is long, and the Alfvén waves carry a strong power, but most of it is trapped in the torus if there is no Alfvén wave filamentation. (b and c) Sketches summarizing the influence of the parallel and perpendicular wavelengths of the power transmission from the Alfvén waves generated near the satellites and the accelerated electrons. The parallel wavelength works on the Alfvén wave transmission through the density gradients, in particular at the torus border, whereas the perpendicular wavelength works on the parallel electric field associated with the Alfvén waves.

(see section 4), the power transfer efficiency from satellite to auroras has to be of the order or larger than 10%.

[12] Such an efficiency has long been regarded as an issue, particularly in the Io case, since early computations [*Wright*, 1987; *Delamere et al.*, 2003] showed that 80% of the Alfvén wave power was reflected back in the torus at the plasma torus boundary, long before reaching the Jovian ionosphere where the acceleration is thought to be located [*Jones and Su*, 2008; *Hess et al.*, 2010] (section 3). The reflection is due to the large gradient of the Alfvén velocity between the inside of the plasma torus and the outside, where the Alfvén velocity is approximately the speed of light. It is also a matter of concern at Europa and Enceladus, since the Alfvén velocities inside their respective plasma tori is lower than that in Io torus. This means that a lower Alfvén velocity in the torus has two opposite effects regarding the power carried by the waves to the planet's ionosphere: (1) increasing the transition regime duration and giving a large power to the Alfvén waves and (2) inducing a reflection of the Alfvén wave power before it can reach the planet ionosphere. Figure 1a shows a sketch of the Alfvénic phase of the interaction (1) when the Alfvén velocity is close to the speed of light and (2) when the Alfvén velocity is far less than the speed of light. In both cases the Alfvénic phase is followed by a steady state current circuit. In the present paper we focus on the intensity of the emissions related to the main Alfvén wave-driven spot only (hereafter MAW), that is before the steady state current is established. We do not discuss the case of the auroral spots generated by the reflected Alfvén waves, since any discussion of such would require a careful description of the interference of the upgoing and downgoing Alfvén waves, including nonlinear behavior [*Jacobsen et al.*, 2007], which is beyond the scope of this analysis.

[13] The interaction resulting in Io's main Alfvén wave driven spot has been solved by a careful computation of the power transmission along the magnetic field line and an estimate of the electron acceleration based on numerical simulations [*Hess et al.*, 2010]. The authors showed that all the features associated with the MAW spot, that is, radio to UV emissions, electron beams and their observed powers, could be explained by assuming that the Alfvén waves generated at Io are filamented before leaving the torus. The purpose of the present paper is to investigate the power transmission between Europa and Jupiter and between Enceladus and Saturn, under the assumption that Alfvén wave filamentation occurs. For that purpose we conduct the same study for Europa and Enceladus that has been conducted for Io by *Hess et al.* [2010]. Equations (1)–(5) give the power generated at the satellites. The transfer model of the Alfvén wave power along the magnetic field lines is presented in section 2. This model is partly based on theoretical considerations, since the only direct observations of filamented Alfvén waves [*Chust et al.*, 2005], although

confirming the Alfvén wave filamentation close to Io, does not sufficiently constrain the parameters of our study.

[14] Contrary to the Io interaction, which has been extensively studied, there are fewer observations available of the Europa and Enceladus interactions. The primary observations constraining the power emitted by these interactions are those of the UV spots. From estimates of their brightness it is possible to estimate the power precipitated in the ionosphere as accelerated electrons [*Gérard and Singh*, 1982; *Gérard et al.*, 2002]. The method we use to estimate the power transmitted from the satellite interaction to the particles and precipitated in the planetary ionosphere is presented in section 3. We then estimate the power emitted in UV from the observed brightness of the satellite footprints, and compare to the results of our model in section 4. The results are discussed in section 5. We show that with a limited set of assumptions (mainly the density profile and the filamentation of the Alfvén wave) we are able to compute a power emitted in UV by these satellite-magnetosphere interactions that is consistent with the observations.

2. Alfvén Wave Propagation

[15] The electric current through the satellites creates a deformation of the nearby magnetic field lines. This deformation can be described as Alfvén waves carrying the current along the planetary magnetic field lines toward the planetary ionosphere. On their way, the Alfvén waves encounter several changes in the plasma parameters, which lead to strong variations of the Alfvén wave phase velocity (e.g., increasing magnetic field flux, plasma torus boundaries, planetary ionosphere…). The Alfvén wave phase velocity is given by:

$$v_{\phi,a}^2 = v_a^2 \frac{\left(1 + k_\perp^2 \rho_s^2\right)}{\left(1 + k_\perp^2 \lambda_e^2\right)} \tag{6}$$

where $k_\perp$ is the perpendicular component of the wave vector $\mathbf{k}$, ρ_s is the ion acoustic gyroradius (kinetic term) and $\lambda_e = c/\omega_{pe}$ is the electron inertial length (inertial term). The variation of the plasma parameters causes the partial reflection of the wave packet as a function of the wavelength. As stated in the introduction, the reflection coefficient of the Alfvén waves may be large and is a critical parameter in understanding satellite-magnetosphere interactions. The reflection coefficient has to be carefully computed in order to estimate the power available for electron acceleration at high latitudes. Early computations used the WKB or the discontinuity approximations, which led to a reflection coefficient that was too low or too high, respectively. These approximations differ in the ratio between the wavelength and the characteristic scale of the phase velocity gradient that they assume (e.g., short wavelength for the WBK approximation and long wavelength for the discontinuity approximation). The WKB approximation gives a reflection coefficient too low to agree with the observed partial trapping of the Alfvén waves inside the torus. The discontinuity approximation gives a reflection coefficient too high to be consistent with the observed intensity of the satellite-related emissions.

[16] The wavelength spectra of the Alfvén waves generated by the satellite-planet interaction covers an intermediate range, which cannot be described by either of the above approximations [*Wright*, 1987]. In the work by *Hess et al.* [2010], the authors developed a new method to compute the reflection coefficient, which is consistent with the WKB approximation for short wavelengths and with the discontinuity approximation for long wavelength. In terms of energy of the wave electromagnetic field, the reflection coefficient approximation by *Hess et al.* [2010] is given by

$$R_\epsilon(s, \mathbf{k}) = \frac{1}{\lambda_\parallel} \left(\int_{s-\frac{\lambda_\parallel}{2}}^{s+\frac{\lambda_\parallel}{2}} \frac{\nabla_s \ln\left(c/v_{\phi,a}(\mathbf{k})\right)}{2} ds \right)^2 \tag{7}$$

which is explicitly dependent on the parallel wavelength ($\lambda_\parallel$), and depends on the perpendicular wavelength through $v_{\phi;a}$ (equation (6)). This equation allows for different reflection coefficients for the Fourier components of the Alfvén wave packet generated at the satellite. Namely, the short wavelengths are slightly reflected whereas the long wavelengths are strongly reflected. The overall reflection is then intermediate between the WKB and discontinuity approximations.

[17] *Hess et al.* [2010] studied the transmission of the Alfvén wave packet along the Io flux tube for a variety of wavelength spectra. The most interesting of which were described by a gaussian and two power laws. The gaussian spectrum corresponds to waves with a satellite length scale $k_0 = \pi/R_{sat}$. This is the simplest distribution expected for a satellite-magnetosphere interaction:

$$f_0(k) = N_0 e^{-\frac{(k-k_0)^2}{2k_0^2}} \tag{8}$$

where N_0 is a normalization coefficient.

[18] The two power law distributions correspond to the turbulent filamentation of the previous gaussian distribution due to the density gradients in the plasma torus [*Champeaux et al.*, 1998; *Sharma et al.*, 2008, and references therein]. The two distributions only differ by their spectral indices. The only published observation of filamented Alfvén waves [*Chust et al.*, 2005], although showing that filamentation exists, was unable to provide an estimate of the spectral index of the Alfvén wave vector distribution, because the observations were realized at frequencies hundreds of times higher than the frequency corresponding to the energy injection scale. The first power law assumes a Kolmogorov cascade, implying a spectral index of −5/3. This kind of cascade is, strictly speaking, only valid for nonmagnetized plasma. For highly magnetized plasma a spectral index of −2 has been theorized by *Galtier et al.* [2000] and *Galtier* [2009]. Such a spectrum has also been observed by *Saur et al.* [2002b] at Saturn. However, the threshold at which the spectral index changes is largely unknown, so we investigate both power laws. Both distributions present a power law spectrum between the energy injection scale k_0 (satellite length scale) and the dissipation (ionic) scale $k_i = \omega_p/(m_i c)$, and are defined by:

$$\begin{aligned} f_{1;\alpha}(k) &= N_1 k_0^{-\alpha} e^{-\frac{(k-k_0)^2}{2k_0^2}} \quad \text{for } k < k_0 \\ f_{1;\alpha}(k) &= N_1 k^{-\alpha} \quad \text{for } k_0 > k > k_I \\ f_{1;\alpha}(k) &= N_1 k_i^{-\alpha} e^{-\frac{(k-k_i)^2}{2k_0^2}} \quad \text{for } k > k_i \end{aligned} \tag{9}$$

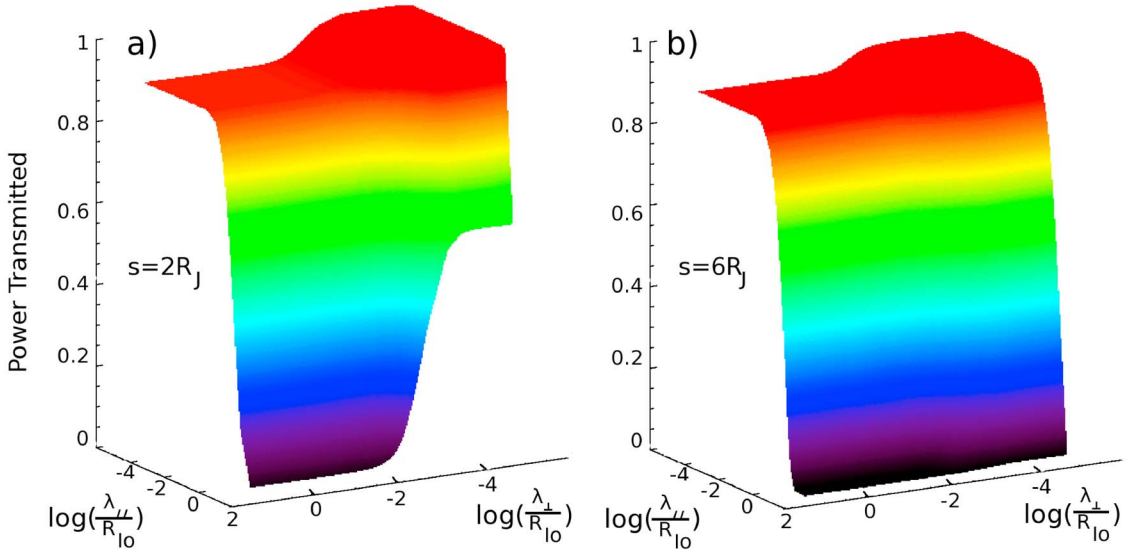

Figure 2. Power transmitted by the Alfvén waves generated at Io at two distances from the torus center versus the parallel and perpendicular wavelengths: (a) s=2 R_J, just outside the torus, and (b) s=6 R_J, near the acceleration region. The wavelengths vary from 20 R_{Io} to 10^{-5} R_{Io}. The long ($\gtrsim R_{Io}$) parallel wavelengths are almost completely reflected.

with N_1 the normalization coefficient, and α = 5/3 or 2 depending on the spectral index we assume for the distribution. The gaussian distribution, which presents long-scale wavelengths compared to the power laws, will be hereafter referred as the long-scale distribution. A realistic distribution can be approximated by:

$$f(k) = a_0 f_0(k) + a_1 f_1(k) \tag{10}$$

The Alfvén wave power transmitted from the satellite to the acceleration region is computed by numerically integrating the Alfvén wave reflection coefficients along the magnetic field lines. Figure 2 shows the relative power of the Alfvén wave transmitted from Io to distances along the Io flux tube corresponding to the torus boundary (Figure 2a) and to the acceleration region (Figure 2b) versus parallel and perpendicular Alfvén wavelengths in the case of the Io interaction (from *Hess et al.* [2010]). The dependance of the power transmission on the parallel wavelength is pronounced. The waves with parallel wavelengths of the order or larger than the satellite radius are almost completely reflected. The perpendicular wavelength plays a less important role, even if smaller wavelengths are slightly less reflected than larger ones.

[19] Figure 3 shows the density profiles used for our computations of the Alfvén phase velocity along the magnetic field lines in the cases of Io, Europa and Enceladus (Figures 3a, 3b, and 3c, respectively). The VIP4 model of the Jovian magnetic field [*Connerney et al.*, 1998] has been used to model the Io and Europa interactions, and the SPV model of the Saturn magnetic field [*Davis and Smith*, 1990] for the Enceladus interaction. The density profiles along the Io and Europa flux tubes were approximated from the torus models of *Bagenal* [1994] and *Moncuquet et al.* [2002], and the ionospheric profile from the simulations by *Su et al.* [2003]. The density profile along the Enceladus flux tube is approximated from torus models [*Sittler et al.*, 2008; *Fleshman et al.*, 2010] and assumes a Saturn ionosphere scale height of ~1600 km.

[20] Table 2 shows the power integrated over the Alfvén wave number k, transmitted along the magnetic field lines from Io, Europa and Enceladus to the acceleration region for the f_0, $f_{1;5/3}$ and $f_{1;2}$ distributions. The power transmission along the magnetic field lines is the smallest for Enceladus and the largest for Io, which is consistent with the Alfvén velocity being the smallest near Enceladus and the largest near Io. The power transmission along the field lines for the long-scale gaussian f_0 distribution varies more than for the power laws $f_{1;\alpha}$ distributions. This is because the power in the f_0 distribution is more concentrated at longer wavelengths, so that a slight increase of the gradient of the Alfvén velocity, which reflects longer wavelengths more strongly, will impact the long-scale distribution more than the power laws. For the three satellite interactions the transmission of the power law distributions is found to be of the order of 40%.

3. Particle Acceleration

[21] Most of the electron acceleration occurs at high latitudes [*Jones and Su*, 2008; *Hess et al.*, 2010] and is due to the parallel electric field associated with the Alfvén waves. The parallel electric field is due to the inertial terms in the Alfvén phase velocity (equation (6)) and thus can be approximated by [*Lysak and Song*, 2003]:

$$\delta E_{\parallel} \simeq \omega_a k_{\perp} \lambda_e^2 \delta B \tag{11}$$

where ω_a is the Alfvén frequency, and δB the magnetic field perturbation associated with the wave. The perpendicular scale is assumed proportional to the flux tube cross section ($k_{\perp} \propto B^{1/2}$), to be consistent with an Alfvén wave propa-

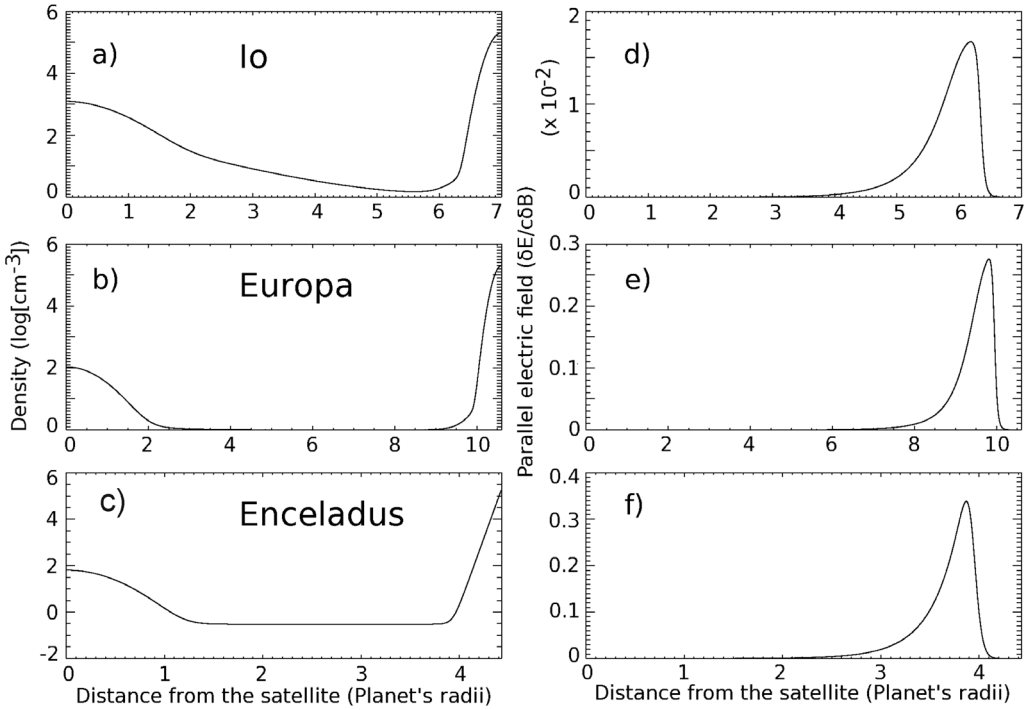

Figure 3. Density profiles along the magnetic field lines used in the present study: (a) Io's flux tube, approximated from torus models [*Bagenal*, 1994; *Moncuquet et al.*, 2002] and simulations [*Su et al.*, 2003] (Ionosphere). (b) Europa's flux tube, approximated from the same models as for Io. (c) Enceladus's flux tube, approximated from torus models [*Sittler et al.*, 2008; *Fleshman et al.*, 2010] and with a Saturn ionosphere height scale ~1600 km. Profiles of the parallel electric field associated with the inertial Alfvén wave as a function of the distance from the satellite for $\lambda_{\parallel} = \lambda_{\perp} = 0.1R_{sat}$. The electric field is normalized to the amplitude of the Alfvén perturbation on the magnetic field δB. It does not take into account the partial reflection of the wave. (d) Io's flux tube, (e) Europa's flux tube, and (f) Enceladus's flux tube.

gating inside a converging flux tube. Smaller perpendicular wavelengths result in stronger acceleration. The parallel electric field profiles for the inertial Alfvén waves peak where the density is low and the magnetic field intense, i.e., just above the region where the ionospheric density increases. This corresponds to altitudes between ~0.5 and ~1 planet radii from the planetary ionosphere [*Hess et al.*, 2010, and references therein]. The exact peak location depends on the planet and satellite involved, specifically the planetary magnetic field model and the ionospheric density

Table 2. Summary of the Power Transmission Through the Torus and of the Efficiency of the Power Transferred to the Particles for Different Distributions of the Alfvén Wavelengths: Io's Case, Europa's Case, and Enceladus's Case

Distribution	Power Escaping the Torus[a] (%)	Power Transferred to the Particles (%)	Power Precipitating on the Main Spot[b] (W)
	Io (Generated Power: ~10^{12} W; Precipitated Power: Few 10^{10} W)		
Long scales	17	9×10^{-3}	$\sim 5 \times 10^{7}$
Kolmogorov	50	5	$\sim 3 \times 10^{10}$
Power law (−2)	45	2	$\sim 10^{10}$
	Europa (Generated Power: ~10^{11} W; Precipitated Power: Few 10^{9} W)		
Long scales	3	2×10^{-3}	$\sim 10^{6}$
Kolmogorov	40	8	$\sim 4 \times 10^{9}$
Power law (−2)	36	3	$\sim 2 \times 10^{9}$
	Enceladus (Generated Power: ~3×10^{8} W; Precipitated Power: 10^{7}–10^{8} W)		
Long scales	5×10^{-3}	4×10^{-5}	~120
Kolmogorov	38	25	$\sim 7.5 \times 10^{7}$
Power law (−2)	34	20	$\sim 6 \times 10^{7}$

[a]Power reaching the acceleration region, i.e., ~1 planetary radius above the planet ionosphere.
[b]For the case of Enceladus, includes the power of the electrons accelerated in the opposite hemisphere which precipitate on the MAW spot, due to the axisymmetric magnetic field of Saturn.

model. Figure 3 shows the profiles of the parallel electric field associated with Alfvén waves whose parallel and perpendicular wavelengths are $\lambda_{\parallel} = \lambda_{\perp} = 0.1$ satellite radii for the cases of Io, Europa and Enceladus (Figures 3d, 3e, and 3f, respectively).

[22] The resonance of the inertial Alfvén wave with the electrons in the auroral regions is considered in many models of particle acceleration at Earth [*Chen et al.*, 2005; *Watt and Rankin*, 2008]. In the terrestrial case, the Alfvén velocity (~0.1 c) is comparable to the particle velocity (1–10 keV, ~0.1 c) so that a resonant wave-particle interaction is possible. However, at Jupiter and Saturn the Alfvén phase velocity (~c) is much larger than the characteristic particle velocities (~0.1 c) due, in part, to the strong planetary magnetic field. Therefore, a resonant interaction is generally not possible, particularly for a wavelength spectrum scaled by the satellite radii. For example, the gradient scale length of the acceleration region shown in Figure 3 is of order 0.1 planetary radii, or ~7000 km in the case of Jupiter. For a given frequency, the parallel wavelength scales as v_a/c, requiring a parallel wavelength of ~10 km at Io. This represents an insignificant fraction of the total wave power for the three distributions discussed above (0.3% at most).

[23] Because most of the wave power in the acceleration region consists of parallel wavelengths ($\lambda_{\parallel}$) on the order of or larger than the gradient scale length of the parallel electric field ($\|\delta E_{\parallel}\|$), we assume that the electron acceleration is due to the limited extent of the electric field. The long parallel wavelengths ensure that electrons accelerated during one phase of the wave can escape the acceleration region before the wave phase changes. In the opposite limit, where $\lambda_{\parallel}$ is negligible relative to the $\|\delta E_{\parallel}\|$ gradient scale length, the electrons would be accelerated and subsequently decelerated with no net particle flux out of the acceleration region. This assumption is fundamental to our estimates of power transmission to the particles described below.

[24] The electron distribution obtained from this acceleration process has an almost unperturbed core with extended tails parallel to B, i.e., a Kappa-like or a beam-like distribution (see discussion by *Hess et al.* [2010]). The acceleration process is independent of the direction of the Alfvén wave propagation, accelerating electrons both toward and away from the planet. This implies the existence of anti-planetward electron beams. The exact shape of the electron distribution may not be computed analytically, but is computed numerically [*Swift*, 2007; *Hess et al.*, 2007, 2010]. The power transferred from the Alfvén wave to the particles is estimated assuming acceleration on half a wave period, at the peak of the parallel electric field profile:

$$P_e = n v_{th} \frac{m}{2} \left(\frac{\pi}{2} \frac{-e\delta E_{\parallel}}{\omega_a m} \right)^2 A = \frac{\pi^2}{8} \frac{\omega_p^2}{\omega_a^2} \epsilon_0 v_{th} \delta E_{\parallel}^2 A \qquad (12)$$

with A the cross section of the flux tube, n the plasma density and v_{th} the electron thermal velocity. The power of the wave on a section of the flux tube is given by the wave's Poynting flux:

$$P_w = \frac{\delta E \times \delta B}{\mu_0} A = \frac{v_{\phi,a} \delta B^2}{\mu_0} A \qquad (13)$$

Using equations (11) and (13), the efficiency of the power transmission to the particles is given by [*Hess et al.*, 2010]:

$$\frac{P_e}{P_w} = \int \min\left(\frac{\pi^2}{8} \frac{v_{th}}{v_{\phi,a}(\mathbf{k})} k_{\perp}^2 \lambda_e^2; 1 \right) T(\mathbf{k}) f(\mathbf{k}) d\mathbf{k} \qquad (14)$$

where $T(\mathbf{k})$ is the Alfvén wave power transfer function computed numerically from equation (7) by integrating the wave reflection coefficient along the magnetic field line. The Alfvén wave transfer function for Io is shown as a function of wavelength in Figure 2. The power transfer efficiency depends not only on the Alfvén wave characteristics and on the magnetic field, but also on the hot plasma density and temperature in the acceleration region. These parameters are not well constrained at Jupiter, nor at Saturn. The temperature for the hot electrons is generally assumed to be a few hundreds of eV in both cases [*Bagenal*, 1994; *Moncuquet et al.*, 2002; *Su et al.*, 2003, 2006; *Fleshman et al.*, 2010]. In the present study we use a thermal velocity $v_{th} = 0.03$ c, which is equivalent to a temperature of 200 eV. Electrons of this energy are not affected by the ambipolar field in the torus, and thus their density is the same in the acceleration region as in the torus. For Jupiter, models predict a density of a few particles per cm^{-3} [*Bagenal*, 1994; *Moncuquet et al.*, 2002]. We use a hot electron density of 1 cm^{-3} for the Io interaction in this analysis. Densities in the Enceladus torus are less constrained. However, models predict that the density of hot electrons in the Enceladus torus is several times lower than at Io. We use a hot electron density of 0.3 cm^{-3} [*Fleshman et al.*, 2010] for the Enceladus interaction.

[25] The efficiency of the power transfer from the satellite interaction to the electrons is shown in Table 2 for the three satellites and the three distribution functions describing the Alfvén wave packet. For each satellite, the long-scale gaussian distribution leads to an acceleration efficiency far lower than that of the power law cases (each of the power law cases having comparable efficiencies). In the power law cases, the acceleration efficiency in the Io interaction case is found to be a few percent (between 4% and 10%). For the Europa interaction, the efficiency is nearly twice as large as in the Io case and in the Enceladus case the efficiency is about six times larger than in the Io case. These differences are explained by the dependence of the power transfer efficiency on $\lambda_e^2 k_{\perp}^2$ (equation (14)), which depends on the interaction parameters as:

$$\lambda_e^2 k_{\perp}^2 \propto \frac{\mu}{n R_{sat}^2} \qquad (15)$$

where μ is the mirror ratio, i.e., the ratio between the magnetic flux at the top of the planet's ionosphere and at the satellite, and n is the density in the acceleration region, i.e., the density of the hot electron population. Thus, smaller satellites generate a more efficient electron acceleration, denser flux tubes generate less efficient acceleration and a larger mirror ratio increases the efficiency.

[26] The larger acceleration efficiency at Europa relative to Io is mostly due to the higher mirror ratio between Europa and the ionosphere, which leads to shorter wavelengths in the acceleration region of the Europa flux tube than in that

of the Io flux tube. In the Enceladus case the acceleration efficiency is six times that of the Io case, but unlike at Europa, the mirror ratio between the satellite and the ionosphere is lower than in Io case (about 8 times lower). Therefore, the increased efficiency is due to both the smaller size of Enceladus (four times smaller than Io), which leads to shorter wavelengths in the acceleration region, and to the lower densities along the flux tube (Table 1).

[27] Since the acceleration occurs in both directions, only half of the power is transmitted to electrons directly precipitating in the ionosphere. The other half forms transhemispheric electron beams (TEB) precipitating in the opposite hemisphere. In the Io interaction case, an UV spot is associated to these beams [*Bonfond et al.*, 2008]. These TEB spots are distinct from the MAW spot in the Io case due to the variations of the MAW lead angle with respect to the Io longitude. These variations are a consequence of the tilt of the Jovian magnetic dipole, which implies that Io is not always in the center of the plasma torus. As the Saturn magnetic dipole is aligned with the rotation axis, such variations do not exist for the Enceladus interaction, so the TEB and MAW spots should merge. The Enceladus footprints must then be powered half by the electron acceleration in their own hemisphere, and half by the electron acceleration in the opposite hemisphere. Hence, electron beams should be observed at the equator in the Enceladus wake, very close to the satellite.

4. Comparison With Observations

[28] The power emitted by the Io interaction can be estimated over a large spectrum of radiation, extending from UV to low-frequency radio. Moreover the plasma environment surrounding Io has been explored by Galileo, unveiling the existence of keV electron beams accelerated close to Jupiter and associated with the main UV spot [*Williams et al.*, 1996, 1999; *Frank and Paterson*, 1999; *Mauk et al.*, 2001]. From these observations, *Hess et al.* [2010] estimated the power transmitted by the main Alfvén wing to the electrons to be a few 10^{10} W, both toward Jupiter and antiplanetward. This is to be compared with the power transferred to the particles in our model. The results of our computations are summarized in Table 2.

[29] In the Io case, powers of a few 10^{10} W are reached for the power law distributions of the Alfvén wave number. Note that as the electrons are accelerated both planetward and antiplanetward, and as some of the particles accelerated toward the planet may be reflected by magnetic mirroring, slightly less than half of the power transferred to the particles is actually precipitated in the planet ionosphere. However, the power of the Io-related emissions is well explained by our model, which assumes that filamentation takes place in the plasma torus.

[30] Concerning the Europa-Jupiter interaction, we can only base our estimate on the brightness of the Europa footprint. This brightness is estimated from HST observations to be ~10 kR on a surface of the order of the Europa cross section projected on the ionosphere. The emitted power inferred from the UV observations is found to be a few 10^8 W [*Clarke et al.*, 2002; *Grodent et al.*, 2006]. Such an emitted power requires, according to the calculation presented by *Gérard and Singh* [1982] and *Gérard et al.* [2002], that the power precipitated as accelerated electrons is a few 10^9 W. The power transmitted to the particles predicted by our model, ~10^9 W (Table 2), is consistent with these analyses. Once again, our model explains the observed brightness of the UV emissions by the filamentation of the Alfvén waves in the equatorial plasma torus, even if half of the power goes to antiplanetward electrons.

[31] The first attempt to observe the Enceladus footprint in the UV was done by *Wannawichian et al.* [2008] using HST. In the absence of finding an Enceladus footprint, *Wannawichian et al.* [2008] determined an upper limit to the brightness of few kR (~10^7 W when integrated over the area of Enceladus as projected on the planet). The UV footprint was finally observed by the Cassini spacecraft with a brightness of ~1 kR [*Pryor et al.*, 2009; W. R. Pryor, personal communication, 2009]. When integrated over a surface corresponding to the cross section of Enceladus projected on the Saturn ionosphere, the observed brightness corresponds to a radiated power of few 10^6 W to 10^7 W in UV. Assuming that the conversion factor from brightness to precipitated power computed for the Io footprint [*Gérard and Singh*, 1982; *Gérard et al.*, 2002] can be applied to the Enceladus footprint (i.e., that the conversion factor at Saturn is the same as the one deduced for the Jovian emissions) the radiated power corresponds to a precipitated power between 10^7 W and 10^8 W.

[32] Our power transfer model predicts a few 10^7 W precipitated for the power law spectra in the case of the Enceladus interaction with the Saturn magnetosphere (Table 2). Hence, the filamentation of the Alfvén waves explains the power emitted in the UV in the case of the Enceladus-Saturn interaction. In the Enceladus case, the electrons accelerated in the antiplanetward direction precipitate on the MAW spot in the opposite hemisphere. Thus, all the power goes to the generation of the main spots.

5. Discussion

5.1. Universality of the Alfvén Wave Filamentation?

[33] For the three cases of satellite-magnetosphere interactions that we have studied, the filamentation of Alfvén waves in the vicinity of the satellites appears to be necessary to explain the observed power emitted in UV from the main Alfvénic spot and, in the case of Io, of radio and infrared emissions as well [*Hess et al.*, 2010]. We conclude that the filamentation of the Alfvén waves is an universal phenomenon, at least in the case of the interactions between unmagnetized satellites and magnetospheres.

[34] The filamentation of the Alfvén waves explains how a large power can escape a plasma torus. The Alfvén velocity inside the torus controls both the duration of the Alfvénic transition regime and its power. The Alfvén wave velocity also affects, in an opposite way, the efficiency of the transmission of the power generated at the satellite to the precipitating electrons. A low Alfvén velocity near the satellite ensures a long and powerful Alfvénic interaction, but it traps the Alfvén waves inside the torus, preventing intense auroral emissions. The filamentation of the Alfvén waves breaks this paradox by allowing the short wavelengths to pass through the torus. Moreover, these short wavelengths accelerate the electrons more efficiently, allowing for intense emissions, even if a large part of the Alfvén wave power

remains trapped in the equatorial plasma torus. Figure 1 summarizes the effects of the shorter parallel and perpendicular wavelength on the power transmission.

[35] As there are no studies of the mechanisms of the Alfvén wave filamentation in the satellite plasma tori, we do not know if the filamentation of the Alfvén wave is a direct consequence of the satellite-magnetosphere interaction, or if it is purely coincidental. The present study shows, however, that intense Alfvénic related emissions (namely UV auroral spots) are a consequence of the Alfvén wave filamentation near the satellites, as intense emissions require a significant power to be generated, i.e., a low Alfvén velocity near the satellite, and a high efficiency of the transmission of this power to the precipitating electrons.

[36] A strong Alfvénic interaction near the satellite without filamentation cannot produce intense UV auroral spots in the ionosphere of the parent planet, but strong UV auroras can nevertheless happen without any filamentation. In this case the auroras would be powered by the steady state current circuit following the Alfvénic transition regime [*Ergun et al.*, 2009]. However, the UV signature for such emission would present continuous auroras, rather than spot-like structures.

5.2. Global Description of the Satellite-Magnetosphere Interaction

[37] Satellite-magnetosphere interactions are predominantly studied in distinct regions: there are studies of the local satellite interactions, of the Alfvén wave propagation, of the electron acceleration, of the auroral emissions, or of the steady state current system. We show in the present paper that these regions are strongly coupled. The Alfvénic regime and steady state current circuit are not two different interactions, but two phases of the same interaction. The transition between these two phases, as well as the power involved, is strongly controlled by the plasma characteristics close to the satellites (that is by the local satellite interactions with the magnetosphere and the torus plasma).

[38] In order to make a more accurate description of the satellite-magnetosphere interaction it is thus necessary to perform simulations of the filamentation in the plasma surrounding the satellites. This medium is difficult to describe, since it involves the interaction between the torus plasma, the satellites and their ionospheres [*Saur et al.*, 1999, 2002a; *Saur*, 2004; *Delamere et al.*, 2003; *Dols et al.*, 2008]. There are thus many nonlinearities, which can permit the filamentation of the Alfvén waves close to the satellite. Moreover, as part of the power generated at the satellite is due to the perturbation of the flow of the plasma torus, Alfvén waves may be directly generated at short wavelengths by this turbulent plasma.

[39] The Alfvénic and steady state current systems are well described, but the understanding of the relaxation of the transient Alfvénic current toward a steady state current requires more study. A better understanding of this relaxation would not only yield important information for satellite-magnetosphere interactions, but also for nonsatellite interactions leading to auroral emissions. In the case of the satellite-magnetosphere interaction, the task is complicated by the interference pattern created in the wake of the satellite [*Jacobsen et al.*, 2007].

[40] The far-field interactions, i.e., the Alfvénic or steady state current interactions with electrons close to the parent planet ionosphere, impact the local satellite interaction through the acceleration of antiplanetward electron beams, that can modify the plasma characteristics close to the satellite [*Saur et al.*, 2002a; *Dols et al.*, 2008; *Fleshman et al.*, 2010], which implies a feedback between the local satellite interaction and the far-field interactions. Describing this feedback is essential in understanding the satellite-magnetosphere interaction.

[41] The next step in the understanding of satellite-magnetosphere interactions is to couple all of the processes taking place. Only then will a global model be able to predict the behavior of any given satellite-magnetosphere interaction.

6. Conclusions

[42] We have investigated the Alfvénic interaction between satellites and the magnetosphere of their parent planet, and discussed the impact of the Alfvén velocity close to the satellite. We showed that a low Alfvén velocity (1) ensures a long and powerful Alfvénic interaction; (2) is responsible for containing the power inside the equatorial plasma torus; and (3) can generate bright emissions only through a turbulent filamentation of the wave, since filamentation permits the power to escape the torus and filamentation leads to generation of a strong parallel electric field at high latitude. The filamentation was already shown to explain the brightness of the Io related emissions [*Hess et al.*, 2010], but the present study shows that it also explains the brightness of the Europa and Enceladus emissions. We compared the Io, Europa and Enceladus interactions and found that (1) the brightness is a function of the mirror ratio for Io and Europa, (2) the acceleration efficiency at Enceladus is nearly 6 times larger than at Io due to the combined effects of a smaller satellite size and of a lower flux tube density, and (3) the power transferred to the electrons at Enceladus would be negligible if there was no filamentation.

[43] Our study suggests that the filamentation of Alfvén waves is a universal process, that occurs at each satellite. However, although [*Chust et al.*, 2005] confirmed Alfvén wave filamentation close to Io , their study was unable to constrain all of the parameters of our study and did not determine the cause of filamentation. Further analysis of in situ measurements near the interacting satellites is thus necessary to confirm the predictions made by our model.

[44] **Acknowledgments.** The authors thank W. R. Pryor for providing the estimate of the power involved in the Enceladus-related aurorae. This work was funded by NASA/OPR grant NNX09AU29G.

[45] Masaki Fujimoto thanks Rudolf Treumann and another reviewer for their assistance in evaluating this paper.

References

Bagenal, F. (1994), Empirical model of the Io plasma torus: Voyager measurements, *J. Geophys. Res.*, *99*, 11,043–11,062.

Bigg, E. K. (1964), Influence of the satellite Io on Jupiter's decametric emission, *Nature*, *203*, 1008–1010.

Bonfond, B., J.-C. Gérard, D. Grodent, and J. Saur (2007), Ultraviolet Io footprint short timescale dynamics, *Geophys. Res. Lett.*, *34*, L06201, doi:10.1029/2006GL028765.

Bonfond, B., D. Grodent, J.-C. Gérard, A. Radioti, J. Saur, and S. Jacobsen (2008), UV Io footprint leading spot: A key feature for understanding the

UV Io footprint multiplicity?, *Geophys. Res. Lett.*, *35*, L05107, doi:10.1029/2007GL032418.
Bonfond, B., D. Grodent, J.-C. Gérard, A. Radioti, V. Dols, P. A. Delamere, and J. T. Clarke (2009), The Io UV footprint: Location, inter-spot distances and tail vertical extent, *J. Geophys. Res.*, *114*, A07224, doi:10.1029/2009JA014312.
Champeaux, S., T. Passot, and P. L. Sulem (1998), Transverse collapse of Alfvén wave-trains with small dispersion, *Phys. Plasmas*, *5*, 100–111.
Chen, L.-J., C. A. Kletzing, S. Hu, and S. R. Bounds (2005), Auroral electron dispersion below inverted-V energies: Resonant deceleration and acceleration by Alfvén waves, *J. Geophys. Res.*, *110*, A10S13, doi:10.1029/2005JA011168.
Chust, T., A. Roux, W. S. Kurth, D. A. Gurnett, M. G. Kivelson, and K. K. Khurana (2005), Are Io's Alfvén wings filamented? Galileo observations, *Planet. Space Sci.*, *53*, 395–412.
Clarke, J. T., et al. (1996), Far-ultraviolet imaging of Jupiter's aurora and the Io "footprint," *Science*, *274*, 404–409.
Clarke, J. T., et al. (2002), Ultraviolet emissions from the magnetic footprints of Io, Ganymede and Europa on Jupiter, *Nature*, *415*, 997–1000.
Connerney, J. E. P., R. Baron, T. Satoh, and T. Owen (1993), Images of excited H_3^+ at the foot of the Io flux tube in Jupiter's atmosphere, *Science*, *262*, 1035–1038.
Connerney, J. E. P., M. H. Acuña, N. F. Ness, and T. Satoh (1998), New models of Jupiter's magnetic field constrained by the Io flux tube footprint, *J. Geophys. Res.*, *103*(12), 11,929–11,940.
Davis, L., Jr., and E. J. Smith (1990), A model of Saturn's magnetic field based on all available data, *J. Geophys. Res.*, *95*, 15,257–15,261, doi:10.1029/JA095iA09p15257.
Delamere, P. A., F. Bagenal, R. Ergun, and Y.-J. Su (2003), Momentum transfer between the Io plasma wake and Jupiter's ionosphere, *J. Geophys. Res.*, *108*(A6), 1241, doi:10.1029/2002JA009530.
Dols, V., P. A. Delamere, and F. Bagenal (2008), A multispecies chemistry model of Io's local interaction with the plasma torus, *J. Geophys. Res.*, *113*, A09208, doi:10.1029/2007JA012805.
Ergun, R. E., L. Ray, P. A. Delamere, F. Bagenal, V. Dols, and Y.-J. Su (2009), Generation of parallel electric fields in the Jupiter-Io torus wake region, *J. Geophys. Res.*, *114*, A05201, doi:10.1029/2008JA013968.
Fleshman, B. L., P. A. Delamere, and F. Bagenal (2010), A sensitivity study of the Enceladus torus, *J. Geophys. Res.*, *115*, E04007, doi:10.1029/2009JE003372.
Frank, L. A., and W. R. Paterson (1999), Intense electron beams observed at Io with the Galileo spacecraft, *J. Geophys. Res.*, *104*, 28,657–28,669.
Galtier, S. (2009), Wave turbulence in magnetized plasmas, *Nonlinear Processes Geophys.*, *16*, 83–98.
Galtier, S., S. V. Nazarenko, A. C. Newell, and A. Pouquet (2000), A weak turbulence theory for incompressible magnetohydrodynamics, *J. Plasma Phys.*, *63*, 447–488.
Gérard, J. C., and V. Singh (1982), A model of energy deposition of energetic electrons and EUV emission in the Jovian and Saturnian atmospheres and implications, *J. Geophys. Res.*, *87*, 4525–4532.
Gérard, J.-C., J. Gustin, D. Grodent, P. Delamere, and J. T. Clarke (2002), Excitation of the FUV Io tail on Jupiter: Characterization of the electron precipitation, *J. Geophys. Res.*, *107*(A11), 1394, doi:10.1029/2002JA009410.
Gérard, J.-C., A. Saglam, D. Grodent, and J. T. Clarke (2006), Morphology of the ultraviolet Io footprint emission and its control by Io's location, *J. Geophys. Res.*, *111*, A04202, doi:10.1029/2005JA011327.
Goertz, C. K. (1983), The Io-control of Jupiter's decametric radiation—The Alfven wave model, *Adv. Space Res.*, *3*, 59–70.
Goldreich, P., and D. Lynden-Bell (1969), Io, a Jovian unipolar inductor, *Astrophys. J.*, *156*, 59–78.
Grodent, D., J.-C. Gérard, J. Gustin, B. H. Mauk, J. E. P. Connerney, and J. T. Clarke (2006), Europa's FUV auroral tail on Jupiter, *Geophys. Res. Lett.*, *33*, L06201, doi:10.1029/2005GL025487.
Grodent, D., B. Bonfond, A. Radioti, J.-C. Gérard, X. Jia, J. D. Nichols, and J. T. Clarke (2009), Auroral footprint of Ganymede, *J. Geophys. Res.*, *114*, A07212, doi:10.1029/2009JA014289.
Hess, S., F. Mottez, and P. Zarka (2007), Jovian S burst generation by Alfvén waves, *J. Geophys. Res.*, *112*, A11212, doi:10.1029/2006JA012191.
Hess, S. L. G., P. Delamere, V. Dols, B. Bonfond, and D. Swift (2010), Power transmission and particle acceleration along the Io flux tube, *J. Geophys. Res.*, *115*, A06205, doi:10.1029/2009JA014928.
Jacobsen, S., F. M. Neubauer, J. Saur, and N. Schilling (2007), Io's nonlinear MHD-wave field in the heterogeneous Jovian magnetosphere, *Geophys. Res. Lett.*, *34*, L10202, doi:10.1029/2006GL029187.
Jones, S. T., and Y.-J. Su (2008), Role of dispersive Alfvén waves in generating parallel electric fields along the Io-Jupiter fluxtube, *J. Geophys. Res.*, *113*, A12205, doi:10.1029/2008JA013512.
Lysak, R. L., and Y. Song (2003), Kinetic theory of the Alfvén wave acceleration of auroral electrons, *J. Geophys. Res.*, *108*(A4), 8005, doi:10.1029/2002JA009406.
Mauk, B. H., D. J. Williams, and A. Eviatar (2001), Understanding Io's space environment interaction: Recent energetic electron measurements from Galileo, *J. Geophys. Res.*, *106*, 26,195–26,208.
Moncuquet, M., F. Bagenal, and N. Meyer-Vernet (2002), Latitudinal structure of outer Io plasma torus, *J. Geophys. Res.*, *107*(A9), 1260, doi:10.1029/2001JA900124.
Neubauer, F. M. (1980), Nonlinear standing Alfven wave current system at Io: Theory, *J. Geophys. Res.*, *85*(14), 1171–1178.
Prangé, R., D. Rego, D. Southwood, P. Zarka, S. Miller, and W. Ip (1996), Rapid energy dissipation and variability of the Io-Jupiter electrodynamic circuit, *Nature*, *379*, 323–325.
Pryor, W. R., et al. (2009), Saturn auroral images and movies from Cassini UVIS, paper presented at Magnetospheres of the Outer Planets, Europlanet, Cologne, Germany.
Saur, J. (2004), A model of Io's local electric field for a combined Alfvénic and unipolar inductor far-field coupling, *J. Geophys. Res.*, *109*, A01210, doi:10.1029/2002JA009354.
Saur, J., and D. F. Strobel (2005), Atmospheres and plasma interactions at Saturn's largest inner icy satellites, *Astrophys. J.*, *620*, L115–L118.
Saur, J., F. M. Neubauer, D. F. Strobel, and M. E. Summers (1999), Three-dimensional plasma simulation of Io's interaction with the Io plasma torus: Asymmetric plasma flow, *J. Geophys. Res.*, *104*, 25,105–25,126.
Saur, J., F. M. Neubauer, D. F. Strobel, and M. E. Summers (2002a), Interpretation of Galileo's Io plasma and field observations: I0, I24, and I27 flybys and close polar passes, *J. Geophys. Res.*, *107*(A12), 1422, doi:10.1029/2001JA005067.
Saur, J., H. Politano, A. Pouquet, and W. H. Matthaeus (2002b), Evidence for weak MHD turbulence in the middle magnetosphere of Jupiter, *Astron. Astrophys.*, *386*, 699–708.
Saur, J., F. M. Neubauer, J. E. P. Connerney, P. Zarka, and M. G. Kivelson (2004), Plasma interaction of Io with its plasma torus, *Jupiter: The Planet, Satellites and Magnetosphere*, pp. 537–560, Cambridge Univ. Press, Cambridge, U. K.
Serio, A. W., and J. T. Clarke (2008), The variation of Io's auroral footprint brightness with the location of Io in the plasma torus, *Icarus*, *197*, 368–374.
Sharma, R. P., M. Malik, and H. D. Singh (2008), Nonlinear theory of kinetic Alfvén waves propagation and multiple filament formation, *Phys. Plasmas*, *15*(6), 062902, doi:10.1063/1.2927445.
Sittler, E. C., et al. (2008), Ion and neutral sources and sinks within Saturn's inner magnetosphere: Cassini results, *Planet. Space Sci.*, *56*, 3–18.
Su, Y.-J., R. E. Ergun, F. Bagenal, and P. A. Delamere (2003), Io-related Jovian auroral arcs: Modeling parallel electric fields, *J. Geophys. Res.*, *108*(A2), 1094, doi:10.1029/2002JA009247.
Su, Y.-J., S. T. Jones, R. E. Ergun, F. Bagenal, S. E. Parker, P. A. Delamere, and R. L. Lysak (2006), Io-Jupiter interaction: Alfvén wave propagation and ionospheric Alfvén resonator, *J. Geophys. Res.*, *111*, A06211, doi:10.1029/2005JA011252.
Swift, D. W. (2007), Simulation of auroral electron acceleration by inertial Alfvén waves, *J. Geophys. Res.*, *112*, A12207, doi:10.1029/2007JA012423.
Wannawichian, S., J. T. Clarke, and D. H. Pontius Jr. (2008), Interaction evidence between Enceladus' atmosphere and Saturn's magnetosphere, *J. Geophys. Res.*, *113*, A07217, doi:10.1029/2007JA012899.
Wannawichian, S., J. T. Clarke, and J. D. Nichols (2010), Ten years of Hubble Space Telescope observations of the variation of the Jovian satellites' auroral footprint brightness, *J. Geophys. Res.*, *115*, A02206, doi:10.1029/2009JA014456.
Watt, C. E. J., and R. Rankin (2008), Electron acceleration and parallel electric fields due to kinetic Alfvén waves in plasma with similar thermal and Alfvén speeds, *Adv. Space Res.*, *42*, 964–969.
Williams, D. J., et al. (1996), Electron beams and ion composition measured at Io and in its torus, *Science*, *274*, 401–403.
Williams, D. J., R. M. Thorne, and B. Mauk (1999), Energetic electron beams and trapped electrons at Io, *J. Geophys. Res.*, *104*, 14,739–14,754.
Wright, A. N. (1987), The interaction of Io's Alfven waves with the Jovian magnetosphere, *J. Geophys. Res.*, *92*, 9963–9970.

P. A. Delamere, V. Dols, S. L. G. Hess, and L. C. Ray, LASP, University of Colorado at Boulder, Boulder, CO 80303, USA. (sebastien.hess@lasp.colorado.edu)